Received: 7 November 2020 | Revised: 27 February 2021 | Accepted: 4 April 2021

IET Power Electronics

DOI: 10.1049/pel2.12141

The Institution of Engineering and Technology WILEY

REVIEW

A state-of-the-art review on topologies and control techniques of solid-state transformers for electric vehicle extreme fast charging

Yameena Tahir[1] | Irfan Khan[2] | Syed Rahman[3] | Muhammad Faisal Nadeem[1] | Atif Iqbal[4] | Yinliang Xu[5] | Mohammad Rafi[4]

[1] Department of Electrical Engineering, University of Engineering and Technology Taxila, Taxila 47080, Pakistan

[2] Clean and Resilient Energy Systems (CARES) Lab, Texas A&M University, Galveston, Texas 77553, USA

[3] Electrical and Computer Engineering Department, Texas A&M University, College Station, Texas, USA

[4] Department of Electrical Engineering, Qatar University, Doha, Qatar

[5] Environmental Science and New Energy Technology Department, Tsinghua-Berkeley Shenzhen Institute, Shenzhen 518055, China

Correspondence
Prof. Atif Iqbal, Department of Electrical Engineering, Qatar University, PO Box 2713, Doha, Qatar.
Email: atif.iqbal@qu.edu.qa

Funding information
UREP, Grant/Award Number: 27-021-2-010; UREP, Grant/Award Number: 27-021-2-010

Abstract

Electrical vehicle (EV) technology has gained popularity due to its higher efficiency, less maintenance, and lower dependence on fossil fuels. However, a longer charging time is a significant barrier to its complete adaptation. Solid state transformer (SST) based extreme fast charging schemes have emerged as an appealing idea with an ability to provide a refuelling capability analogous to that of gasoline vehicles. Therefore, this paper reviews the EV charger requirements, specifications, and design criteria for high power applications. At first, the key barriers of using a traditional low frequency transformer (LFT) are discussed, and potential solutions are suggested by replacing the conventional LFT with high frequency SST at extreme fast-charging (XFC) stations. Then, various SST-based converter topologies and their control for EV fast-charging stations are described. The reviewed control strategies are compared while considering several factors such as harmonics, voltage drop under varying loading conditions, dc offset load unbalances, overloads, and protection against system disturbances. Furthermore, the realization of SST for EV charging is comprehensively discussed, which facilitates understanding the current challenges, based on which potential solutions are also suggested.

1 | INTRODUCTION

The transportation sector and electricity generation explicate for more than 60% of the primary world-wide energy demand [1]. Since fossil fuels are the primary source of energy for the transportation sector, their contribution to the immense air pollution and greenhouse gas emissions has increased environmental concerns. Transportation sector organizations aim to adapt EVs into the up-to-date power grids to operate a clean energy viewpoint [2]. With the large-scale development of the EVs, a significant reduction in the use of petroleum, greenhouse gas emissions, and fossil fuel dependence has been observed [3]. Nonetheless, despite the growth of EVs, scarcity in charging infrastructures, extended charging times, range anxiety, and existing battery technologies may limit EVs applicability to short length trips. Therefore, there is an essential requirement of a cost-effective, efficient, and reliable infrastructure for EV charging stations that can compete with the present gasoline vehicle refuelling infrastructure. Figure 1 shows the driving range for commercially available EVs in the industry [4–7]. It is evident from the figure that advanced research work has been done to deliver a driving range of more than 200 miles. However, EV chargers with a rating higher than 350 kW can refuel EVs in less than 10 min [8].

EV chargers can be categorized into two types: 1) on-board, and 2) off-board chargers. Conventional on-board charger

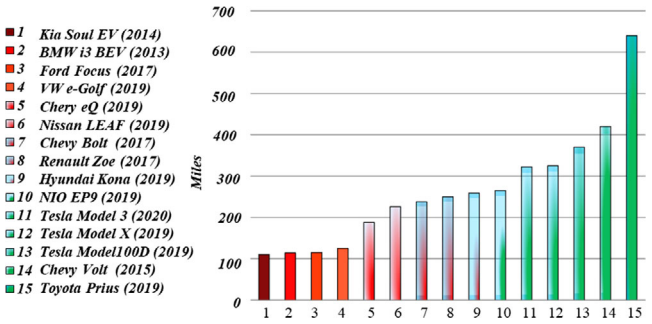

FIGURE 1 Range of EVs in miles (charged at a constant rated power) [4–7]

power ratings are restricted due to the cost, space, and weight restraints [9–12]. The accessibility of charging infrastructure diminishes on-board energy storage necessities and costs. An off-board charger is, however, intended for high rates of charging and is less constrained by size or weight [12]. Most of the primitive EV charger designs are unidirectional in nature that can reduce hardware constraint and interconnection problems [13, 14]. In the existing literature, EV charging strategies include constant voltage (CV) and constant current (CC) charging. A combination of CCCV mode combines the positive outcomes of both methods and is the most optimal method in EV fast charging. However, the projected rise in the number of EVs [8] may result in an increase of a significant amount of load on the utility grid due to the charging of batteries inside them. At the same time, batteries may also support the utility grid by injecting power back into the power grid during peak load demand (Vehicle-2-Grid (V2G) Mode) [15, 16]. With the intended operation in V2G mode, benefits such as peak load shaving, economic power flow, load flattening, and power system stability enhancement may be achieved [17]. Moreover, some major factors of the grid side such as efficiency, reliability, losses, and stability of the grid, are also improved by the V2G system, as proved in [17].

For harnessing this power, bidirectional power flow is implemented [18]. Bidirectional chargers must be developed to seamlessly manage power flow in both directions, with an insignificant difference in efficiency and performance [19–21]. The pros and cons of high-power bidirectional converters for EV charging applications are compared in [19].

Apart from a large number of positive outcomes of dc fast chargers, their adverse effects on the grid can be mitigated by providing the control of the EV charging station's peak demand to the utility. The overloading and voltage variations of feeders beyond the allowable limits are observed in recent literature due to the single point excessive load [22]. To reduce the power quality issues, the charging station can provide ancillary services to the grid by utilizing power factor control (PFC) and the V2G bidirectional power flow. Further, the voltage control problem [23] of utility can also be solved by the injection of reactive power back to the grid with the help of a multi-MVA charging station. The constraints are given in the modified IEEE 1547–2018 standard [24].

State of the art extreme fast chargers (XFCs) require line frequency transformers to convert medium voltage (MV) ac input to low voltage (LV) ac output. The issues of large size, high installation cost, and power losses due to the usage of conventional low frequency transformer can be addressed by the state-of-the-art SST-based XFCs system [25–28]. The SST-based fast charging solution provides galvanic isolation, reactive power control, voltage regulation, and easy integration of renewable energy systems (RESs) with reduced overall cost and size considerations. Moreover, for high power XFC applications, modular SST configuration with input series and output parallel combination is adopted. However, the complete adoption of such infrastructure requires advanced converter topologies, control techniques, proper protection schemes, standards, and other technical challenges [29]. Various XFC converter topologies appropriate for SST applications are presented in the literature [8, 19, 30, 31, 33].

This paper reviews the EV charging requirements, specifications, and design criteria for high power applications. The key barriers of using traditional low frequency transformer are discussed, and the potential solutions are provided in replacing the conventional (line frequency) transformer with high frequency SST in XFC stations. Recent MV SST developments and topologies are discussed with reference to EV extreme fast charging stations. Moreover, the advantages and disadvantages of the modular nature of SST-based XFC stations are also included. Different SST converter topologies have been presented for fast charging applications proposed in the literature. In comparison with [8, 30, 31, 33], apart from various SST-based converter topologies for XFC applications, their control for EV fast charging stations is described. The reviewed control strategies are compared while considering several factors such as harmonics, voltage drop under varying loading conditions, dc offset load unbalances, overloads, and protection against system disturbances. Furthermore, we outline the future challenges and their proposed solutions in the complete adoption of SSTs in XFCs.

The rest of the paper is organized as follows. The high-power requirements for EV fast chargers are discussed in Section 2. The high frequency SST as the potential solution for high power EV fast-charging stations is identified in Section 3. Section 4 describes the recent topologies of the SST-based XFC system, while in Section 5, MV SST-based XFC charging station's converter designs and their control is given. Then, the future challenges to the adoption of SST-based solutions are discussed, and their potential solutions are presented in Section 6. Finally, Section 7 provides the concluding remarks.

2 | EV CHARGER SPECIFICATIONS FOR HIGH POWER REQUIREMENT

Level 1 and level 2 ac on-board chargers are capable of supplying power of 1.9 and 19.2 kW, respectively [32–34], as shown in Table 1. These chargers are limited to night charging (domestic charging) because of their comparatively low power ratings. For adding 200 miles of driving range to the EV battery, an

TABLE 1 Different charging power level [35]

Power levels	Voltage level	Rated power (kW)	Charging time
Level 1On-board1-phase(Opportunity)	120 V_{ac}230 V_{ac}	1.4 (12 A)1.9 (20 A)	4–11 h11–36 h
Level 2On-board1 or 3-phase(Primary)	240 V_{ac}400 V_{ac}	4 (17 A)8 (32 A)19.2 (80 A)	1–4 h2–6 h2–3 h
Level 3Off-board3-phase(Fast)	208–600 V_{ac} or V_{dc}	50100up to 350	0.4–1 h0.2–0.5 h <0.167 h

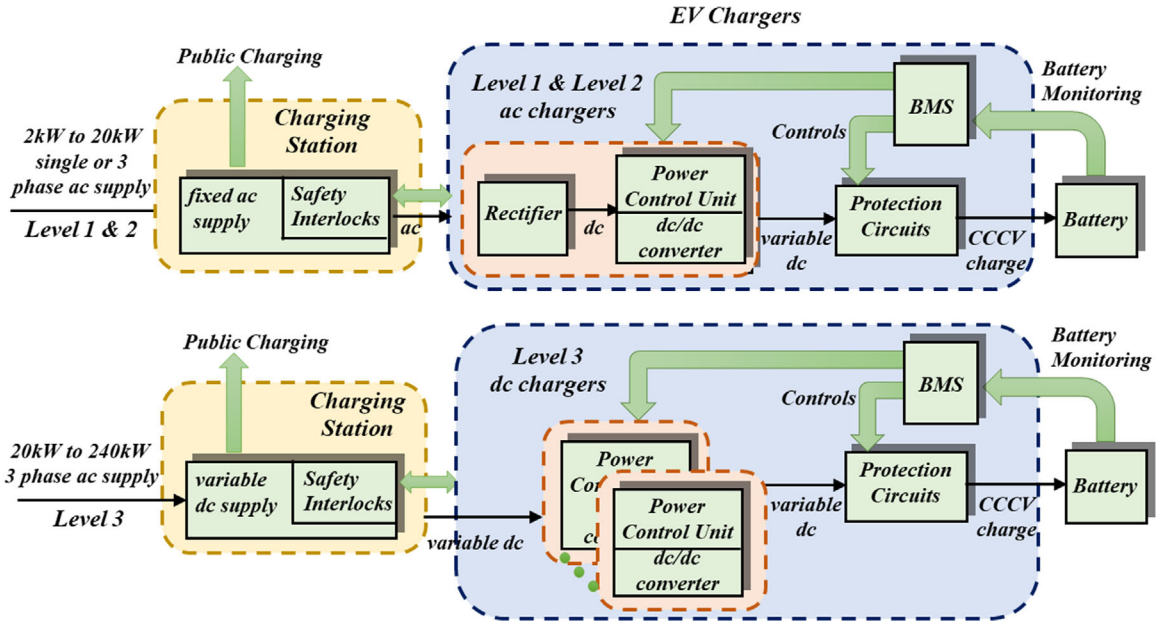

FIGURE 2 Block diagram of the electrical parts used in Level 1, 2 and 3 EV charging [33]

on-board 240 V plug takes more than 8 h. So, it is inappropriate for longer journeys and causes range anxiety. This issue leads to the evolution of dc fast chargers, rated at power levels up to 350 kW nowadays. Such off-board chargers deliver power to the EV's battery through an isolated power converter from outside the vehicle in a relatively shorter charging time. The major advantage of the off-board charger is that it is less constrained by size and weight while providing the fastest charging time, as is evident from the charging time data given in Table 1 [35]. There are currently several fast charging standards, such as CHAdeMO 3.0, that enable dc charging with a power level above 500 kW (with a maximum current of 600 A) [36].

Figure 2 shows the block diagram of the electrical parts used in Level 1, 2, and 3 EV charging. All three charging systems take ac power from the grid and convert it into the desired voltage level for charging purposes. In EV charging applications, Level 1 and Level 2 chargers are entirely confined within the vehicle (except for bicycles). However, in Level 3 charging, the functions are divided between the charging station and the EV's on-board charger. The commonly used converter topologies in these EV charging levels include unidirectional and bidirectional isolated or non-isolated configurations. Level 1,2 charging works from a single-phase or three-phase ac power outlet, while level 3 charging works on three-phase ac supply with same functionality as level 1,2 charging but with high power level. The power control unit in Figure 2 represents the control algorithms adopted by these charging levels. They include PI controller, PID controller, fuzzy logic, adaptive, sliding mode and neural network controllers [33]. Furthermore, the protection measures in low power charging is relatively simple and can easily controlled through a circuit breaker and a current-interrupting device (CID). However, the safety measures in high power charging are managed by the charger itself and the battery management system (BMS).

In the process of EV charging, the information is first exchanged between the charger and the vehicle, e.g. the desired reference of current and voltage. The battery management system modifies the charger's current based on parameters such as the state of charge (SOC) of the battery. By examining the SOC, the EV is able to stop the charging by setting the charging current to zero. EV battery then isolates itself from the charger with the help of a dc contactor. Generally, EV charging strategies include CV and CC charging methods. Moreover, constant current, constant voltage (CCCV) charging profile is more optimal in the charging method and is often followed by EV batteries (Figure 2). Several strategies are proposed in the literature concerning the fast charge problem to obtain CCCV [37–39]. A model predictive controller is one of the most

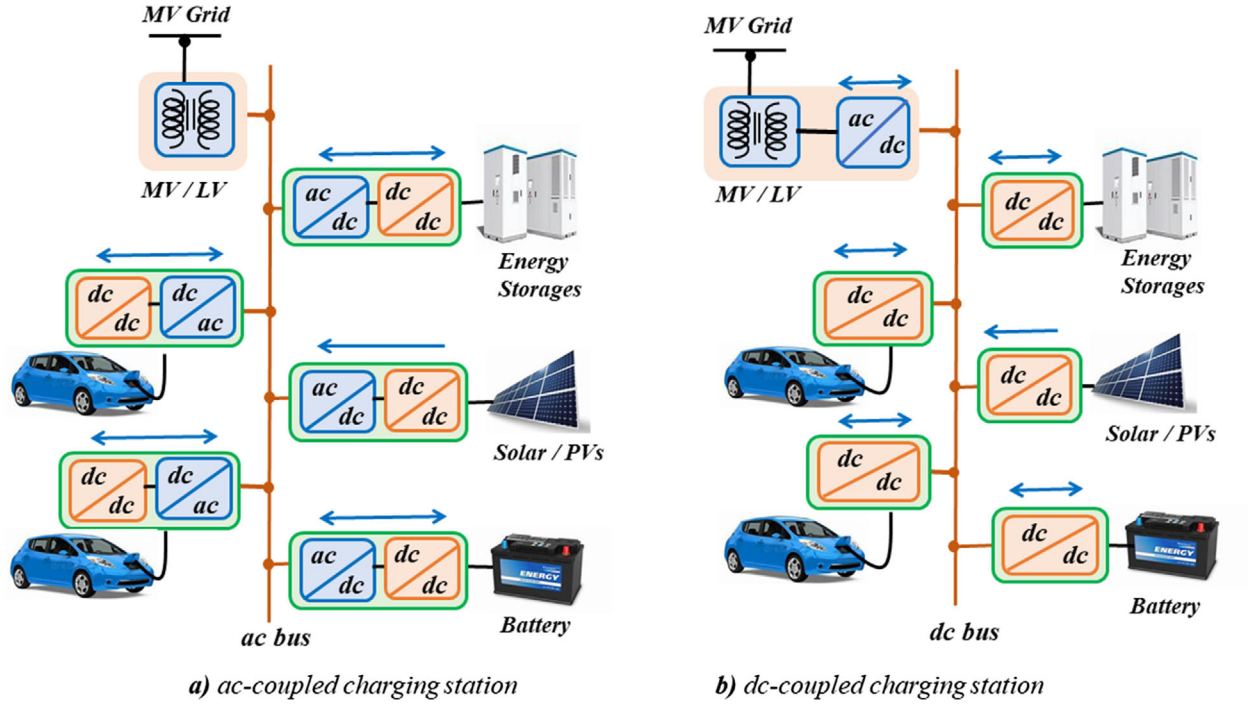

FIGURE 3 Extreme fast charging configurations using LV transformer. (a) Ac-coupled charging station, (b) dc-coupled charging station

popular frameworks to produce a well-known CCCV profile when subjected to real-world constraints. The conventional fast charge problem comprises of computing the input current profile that can bring the initial SOC to final SOC in minimum possible time as illustrated in Equations (1)–(3) [40, 41]:

$$min_I \left[time\ to\ charge\right]_{SOC_o \rightarrow SOC_f} \tag{1}$$

$$min_I = \sum_{i=0}^{N} \left(SOC\ (k+ik) - SOC_{ref}\right)^2 \tag{2}$$

$$(SOC\ (k+ik) \leq SOC_{max}) \tag{3}$$

In the CC region, the battery voltage increases with the SOC during the charging process, increasing the power acceptance by the battery pack. As soon as the CV period initiates, the charge current reduces to retain the CV, thereby reduces the delivered power at the battery terminals. As a consequence, the rate of charge of the battery also reduced during CV phase [8].

Typically, available dc fast chargers utilize two stages of power electronics conversion: the first stage involves the conversion of three-phase ac to medium volts dc termed as rectification, along with PFC, and the second stage converts the medium dc voltage into a regulated dc voltage, matching with EV battery ratings. The galvanic isolation provides separation between the vehicle and the grid, it further permits the parallel connection of the output stages of the charger in order to meet the high-power requirements. For example, Tesla Supercharger (135 kW) was made by combining 12 paralleled modules/converters [42].

Since the EV fast chargers are defined to operate similarly to the gas stations, designing multiple charging nodes is necessary for a charging infrastructure supplying multiple vehicles. Presently, an ac-coupled system illustrated in Figure 3(a) can be seen in multiport charging stations. The ac-connected approach's benefits are rectifier/inverter technology, availability of ac switchgear, protection devices, and standardized protocols for EV fast-charging stations [43–45].

The major drawback in the ac-connected system is the higher number of power electronic converters that increase the system's cost and complexity, thereby reducing efficiency. In the case of a dc-connected system (Figure 3(b)), a three-phase transformer supplies power to a low voltage rectifier, which delivers dc power supply to the standalone sub-stations. This approach reduces the conversion stages and involves the incorporation of RESs. However, dc protection schemes and standards are required for the development of such a system. However, both of the above-mentioned systems require a three-phase step-down transformer that provides LV power supply as well as galvanic isolation. Table 2 enlists the specifications of top-selling EV fast chargers available in the market.

It is illustrated in Table 2 that a 50-kW fast charger requires 72 min to add 200 miles of range in comparison, the 135 kW Tesla Supercharger only needs 27 min [30]. ABB Terra HP (350 kW) dc super-fast charger takes only 10 min for the same purpose, thus mimics the refuelling experience of gasoline vehicles. As the rated power of the EV charger goes on increasing, the weight and volume also increase. Therefore, for high power applications, there is a need to reduce the size of the charger. Furthermore, the public and workplace charging infrastructure hardware costs comprise of the charger and its pedestal. Based on the average hardware costs from various studies for the dc fast chargers, the range of cost for 50 kW dc fast charger is given as $20,000 to $35,800, for 150 kW fast charger, the cost is

TABLE 2 Specifications for DC fast-charges [30, 31]

Model	Rated power (kW)	Based on standards	Vol. (L)	Weight (kg)	Input voltage	Output dc voltage (V)	Output dc current (A)	Peak efficiency	Time to add 200 mi (min)
Tritium Veefil-RT [46, 47]	50	CSS Types 1 and 2 CHAdeMO 1.0	495	165	380–480 V_{ac} 600–900 V_{dc}	200–500 50–500	125	>92%	72
Takaoka Toko HFR1-50B [48]	50	CHAdeMO 2.0	662	210	200 V_{ac}	150–450	125	90%	70
PHIHONG Integrated type [49]	120	GB/T	591	240	380 V_{ac} ± 15% 480 V_{ac} ± 15%	200–750	240	93.5%	30
Tesla supercharger [50]	135	Supercharger	1047	600	380–480 V_{ac}	50–410	330	92%	27
EVTEC expresso and charge [51]	150	SAE Combo 1 CHAdeMO 1.0	1581	400	400 V_{ac} ± 15%	170–500	300	93%	24
ABB Terra HP [52]	350	SAE Combo 1 CHAdeMO 1.2	1894	1340	400 V_{ac} ± 15%	150–920	375	95%	10

$75,600 to $100,000 while for 350 kW dc fast charger, the range of cost is $128,000 to $150,000.

Advanced dc fast chargers for electric vehicles are properly configured to directly connect with a three-phase power supply, having 480V line-to-line voltage, since it is generally inaccessible in public installations. Therefore, a dedicated low frequency MV to LV transformer is used to supply three-phase power to EV fast-charging stations, minimize the distribution network, and provide galvanic isolation. This bulky transformer increases the size and cost and adds complexity to the installation [44]. Additionally, the applications of low frequency, high power transformers require huge conductors and bulky switchgear/protection instruments. Furthermore, a confined concrete foundation is required for the transformer; thereby, installation costs are also increased. This results in a high-priced charging system that requires evidential infrastructure [8]. The current advanced grid control requires a fast response from all entities connected to it, which may not be possible with traditional line frequency transformers. Moreover, other issues relating to LFT include RES integration, grid current harmonics, voltage regulation problems, additional heating losses, and reactive power control problems.

3 | SOLID-STATE TRANSFORMER—A SOLUTION FOR HIGH POWER EV EXTREME FAST-CHARGING

The state-of-art concept to overcome the aforementioned issues is the utilization of SST [53] technology to XFC architectures, which is already being used in distribution systems [29] and railway traction systems [7]. This approach eliminates the need for grid-frequency MV to LV transformer that can interface with the medium voltage grid directly. In addition to the step-down function, it provides galvanic isolation, reactive power control, better power quality performance, voltage regulation, and easy integration of RES [54]. Furthermore, the overall cost and size of SST are comparatively less than LFT [25]. An SST-based solution can be designed to provide either unidirectional or bidirectional power flow that better regulates the active and reactive power, in addition to offering V2G function. Moreover, it performs PFC function along with protection features such as fault current limitation and isolation. The SST-based EV charging station includes a common dc bus to introduce an interface among RESs, battery energy storage systems (BESSs), and EVs through dc/dc converters, thereby ensures fewer conversion stages and higher efficiency [53].

In the context of XFC in SST, galvanic isolation is achieved by using a high frequency transformer (HFT). The HFT operates at a much higher frequency than the LV line frequency transformer. Owing to high frequency operation in SST, the size of the transformer reduces significantly, resulting in evidential space savings. The reduced size leads to lower system installation costs by at least 40% compared to the traditional solution [19]. The installation cost of the charging station is comprehensively reduced by using SST based solution; however, it has been shown in the literature that the material cost of MV SST

TABLE 3 Comparison of LFT and SST-based XFC stations [7, 31]

Parameters	LFT-based XFC	SST-based XFC
Reliability	More	Less
Cost	High	Low
Flexibility	Less	More
Technical maturity	High	Low
Control	Simple	Control
Protection	Straightforward	Complex

is five times higher than LFT [54, 55]. A comprehensive comparison between LFT and SST-based XFC stations is shown in Table 3. The power losses of MV SST are half due to a relatively smaller transformer size, whereas the weight and volume are reduced to almost one third, as compared to the LFT system [54]. For example, a comprehensive comparison between LFT and an increase of 7% (from 91.5% to 98.5%) in the system efficiency at 1 MW power would reduce the power losses from 85 to 15 kW. The direct connection with the MV line also causes the reduction of electricity costs.

In densely populated areas, installed EV fast charger with reduced system size can provide more power, i.e. better site utilization. On the same footprint, a higher number of charging points can be achieved with SST. This results in higher availability of charging points that reduce waiting time and lead to faster and economical charging experiences [60]. A comparison of Tesla's supercharger station is made with the SST-based solution for the same power ratings in [8, 30], which shows a much smaller footprint for the SST-based solution. The potentially lower losses of the SST-based system that lead to power savings for the charging station owners originate mainly from the rectification at a higher voltage, and hence lower currents, especially in the case of multi-level topologies, which allow reducing the device switching frequencies. Due to the elimination of harmonic current by pulse width modulated (PWM) rectifier on the input side of SST, power losses are reduced. The minimum value of the input side filter can be found by using the Equation (4) [61]:

$$L_f = \frac{T_{sw} V_{dc}}{\Delta i_{f,max}} \left(1 - M\sin\left(\omega_g t\right)\right) M\sin\left(\omega_g t\right) \tag{4}$$

where M is modulation amplitude, T_{sw} is switching period, and ω_g is the grid side frequency. However, this feature is not available in LFT.

Furthermore, to interface with the MV grid directly, multi-module-based SSTs are commonly used to attain the desired power and voltage levels. Due to SST's nature, additional SST modules can be added to the existing structure for higher power requirements. But, in traditional LFT based charging stations, any extension of charging capabilities requires transformers replacement. Despite the many benefits of the high voltage and high-power SST approach, its design and implementation are challenging. Therefore, considerable effort is required for the rapid growth of the SST in XFC stations. Hence, many developments in this area can be found in past decades. A technical comparison of several XFC methodologies presently existing in the different parts of the world is given in Table 4. A comparison of SST designs and topologies is presented in [26, 27].

4 | MV SST-BASED XFC STATIONS RECENT DEVELOPMENTS AND TOPOLOGIES

Several isolated power converter topologies suitable for SST applications are presented in the literature [62, 63]. There are four possible topological configurations with a primary focus on the conversion stages, as shown in Figure 4 [26]. Numerous SST-based EV charging stations include power converter stages that ensure higher efficiency with more reliability. A single-stage SST topology [64, 65], as illustrated in Figure 4(a) involves ac/ac conversion with an isolated HFT link. A dc/dc converter is used at the load end to obtain a desired dc voltage level for the particular EV. The use of HFT provides galvanic isolation and reduces the system's size and cost, as discussed in sections II and III. Due to the unavailability of a dedicated dc-link on the input side, it may not offer PFC, reactive power compensation, and bidirectional power flow for an EV charging application. Furthermore, the voltage conversion ratio and switching frequency of this topology are low due to the available technology in the 1970s [53]. An ac/ac converter for SST is proposed in [66] that allows bidirectional power flow. The control of single-stage SST topology is simple, but due to the absence of dc link, it limits the functionality of SST.

In contrast to type I SST, type II SST uses a two-stage topology that includes an isolated ac/dc conversion stage and provides an LVDC link [67–69]. Due to this DC link (Figure 4(b)), the two-stage SST can perform reactive power compensation by selecting proper topologies. Furthermore, the LVDC link's availability also makes the feasibility of renewable energy integration possible at the LV side [70]. However, type I and II topologies are inappropriate for high voltage applications. This is due to the reason that complex and multi-level configurations cannot be applied at the high voltage side easily. Moreover, in such a wide input power range, the zero-voltage switching (ZVS) is difficult to be assured. Further, high switching losses that may lead to lower efficiency are the major challenges of the above-mentioned topologies. Another way to attain a two-stage conversion is to replace the LVDC link with the HVDC link (illustrated in Figure 4(c)) [71, 62]. In this type, due to the availability of a dedicated ac/dc converter and an HVDC link (PWM rectifier), PFC can be realized. Several studies on ac/dc converter configurations result in improved power quality in the context of PFC, reduced THD, and voltage regulation with unidirectional and bidirectional power flow [13]. Additionally, it is possible to achieve soft switching (zero voltage switching) by using a resonant converter [53]. Nevertheless, renewable energy integration is not possible at the LV side due to the unavailability of the LVDC link. Since a high voltage and high-power source is required for XFC chargers, type I, II, and III topologies are not suitable for this application. This unsuitability is due to high

TABLE 4 Technical comparison of XFC stations

Model	Rated power (kW)	Output interfaces	Dimensions (H × W × D) (mm)	Weight (kg)	User authentication	Peak efficiency	Available region	Vehicles charged
Delta UFC 150 kW [56]	150	CSS 2 CHAdeMO IEC 62196-2 Type 2	2079 × 852 × 998	500	ISO/IEC 14443 RFID card reader	95%	Europe	Tesla Model S and Model X vehicles
ABB Terra 184 [57]	180	CSS 1 or CSS 2 ChAdeMO 1.2	1900 × 565 × 880	365	ISO/IEC 14443A/B, ISO/IEC 15393	95%	North America	Mitsubishi Outlander P-HEV
Delta UFC 200 [58]	200	CSS CHAdeMO	2079 × 859 × 998	450	RFID and NFC credit card, ISO 15118	94%	United Kingdom	BMW i3
ABB Terra HP 350 [57]	350	CCS 1 CHAdeMO	2030 × 1170 × 770	1340	ISO/IEC 14443A/B, ISO/IEC 15393	95%	North America	Zero Motorcycles
Rhombus RES-OCS-500 [59]	500	CCS 1	2336 × 2616 × 965	1587	OCPP1.6 and Rhombus VectorStat	>95%	USA	Jaguar I-Pace

switching losses (when operating at high switching frequency), resulting in low efficiency. To overcome these problems, type IV topology (Figure 4(d)) consists of three-stage conversion with HFT dc/dc isolation, includes both HVDC and LVDC links at the primary and secondary side, respectively [61, 72]. Table 5 shows a comparison of SST topologies in the context of cost, size, and modularity implementation.

The first stage consists of an ac/dc rectifier with an HVDC link. It shapes the input current, provides bidirectional power flow along with reactive power compensation [73–76] and harmonic elimination [77–79]. The second stage consists of HFT to provide galvanic isolation, and the DAB converter is used to regulate the active power flow. In the final stage, the stepped-down voltage is transferred to the LVDC bus, and the voltage is shaped to 50/60 Hz waveform at the load side where EV is charged, and the desired voltage level is achieved using dc/dc converter. Most SSTs adopt the type IV topology to provide an optimized performance in the context of size, weight, volume, and efficiency.

The most prominent reason for the popularity of type IV topology is its modular nature [80]. In such a modular configuration, the input stages are connected in series to enhance the voltage blocking capability, whereas, in order to provide a large output current at a desired dc voltage level, the module outputs are connected in parallel, as shown in Figure 5. This design can be used for high voltage and high -power applications. Moreover, if the power and voltage requirement rise in the future, the complete replacement of the whole system can be avoided by adding the required stages/modules but keeping a check on the balanced voltage sharing at the input side. Moreover, a suitable voltage and/or current control is required for the regulation of voltage and current [77, 82]. This topology utilizes low voltage switches (MOSFETs or IGBTs) for the XFC operation and has the potential to reduce the size of the passive filter. However, this configuration uses a large number of components that increase the system size, which further leads to lower reliability [30, 81, 83–85].

5 | MV SST-BASED XFC STATIONS CONVERTER DESIGNS AND THEIR CONTROL

The idea of SST was initiated in 1968 [87]. However, it took more than 50 years to develop the desired semiconductor devices for MV SST's proper functionality. The accessibility of contemporary power electronics devices (such as IGBTs and SiCs), is a key enabler for MV SST applications. Due to the rapid advancement of high voltage SiC MOSFETs, the direct integration of SST with the MV grid is performed using a single module converter (SMC). The SMC has higher system efficiency, reliability and it remarkably reduces the complexity of the system. Table 6 gives a comparison of MV interfaced SST-based XFC prototypes. A few of them are explained below.

A SiC MOSFETs and JBS (junction barrier Schottky) diodes based 13 kV single module SST design is proposed and implemented in [61, 88] for direct interfacing with 3.6 kV MV grid

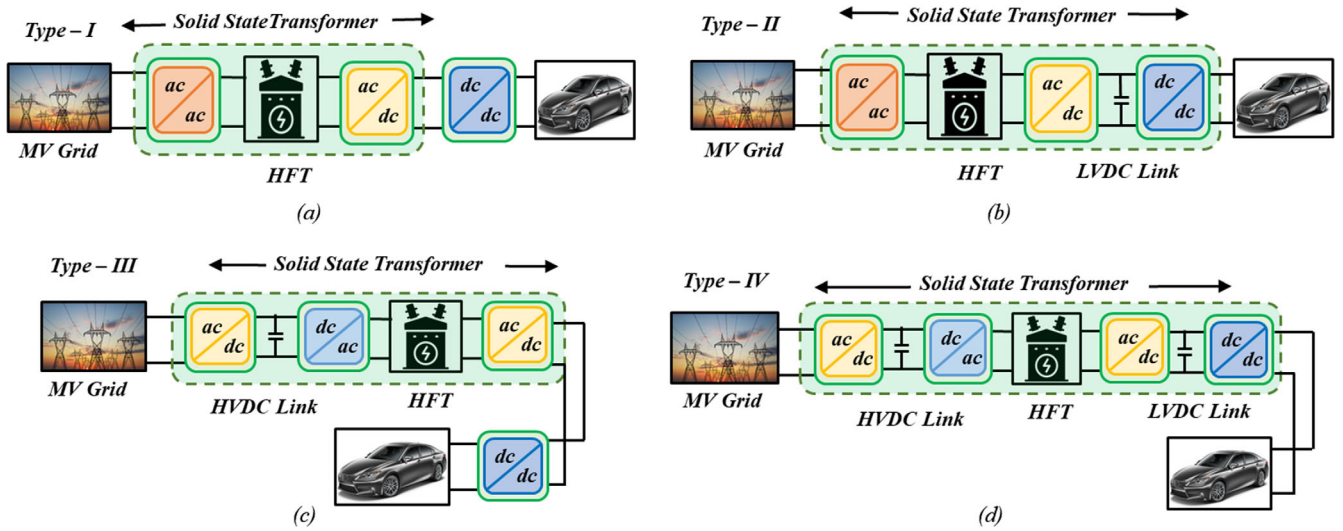

FIGURE 4 SST-based topologies for EV fast charging stations, (a) single-stage topology with HFT, (b) two-stages with LVDC link, (c) two-stages with HVDC link, (d) three-stages with LVDC and HVDC links

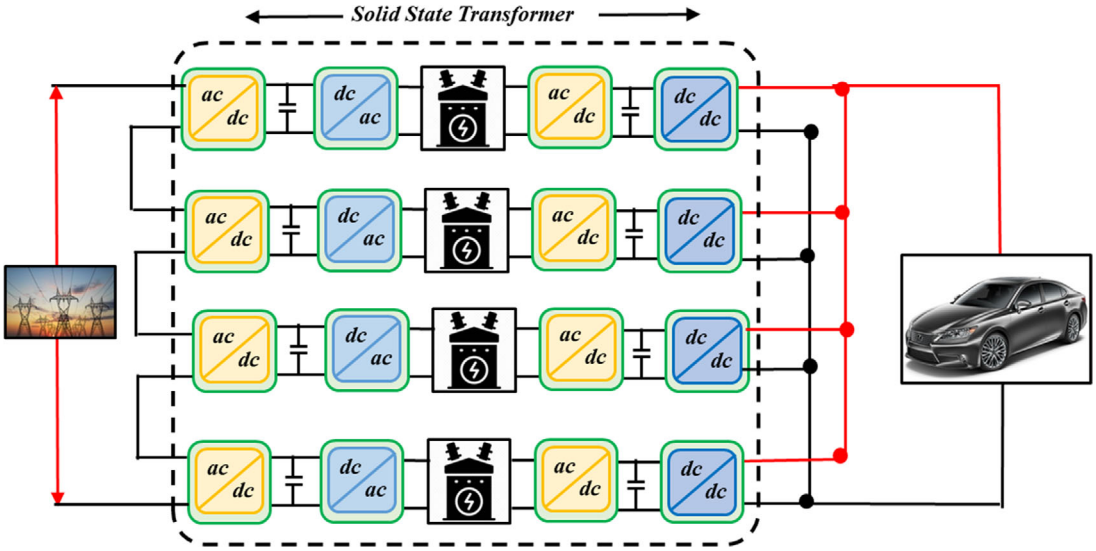

FIGURE 5 Modular design of type IV SST-based XFC with four modules for high voltage and high power EV charging

as shown in Figure 6(a). In this module, the ac/dc front end comprises a single H-bridge with an LCL filter for the regulation of grid-side current. However, the reduction in switching losses of ac/dc rectifier is achieved by employing a unipolar PWM modulation strategy with its one leg operating as an unfolding bridge, while the switching frequency is limited to 6 kHz. A similar design with an LCL filter was used by ABB's fast charging for EVs [89]. The isolated dc/dc stage includes the dual half-bridge (DHB) converter to achieve ZVS for the high-power conversion. The HFT of the DHB dc/dc stage is designed to achieve maximum soft-switching range and high voltage insulation. For SiC SST, the conversion of MV to LV at the secondary side is achieved with an HFT turn ratio of 15.

Phase shift controller design, as mentioned in Figure 6(b), is used to regulate the output voltage and achieve ZVS for all the MOSFETs. The per-unit expression for the power delivered at a specific phase angle ¢ and the output current, from MV to LV side for the DHB, is given by Equations (5) and (6), respectively [88].

$$P_{p.u} = I_{b,p.u} = \frac{d\varphi\,(\pi - |\varphi|)}{\pi} \tag{5}$$

$$I_{l,p.u} = \frac{n\varphi\,(\pi - |\varphi|)}{\pi} \tag{6}$$

Equation (5) shows that the steady-state output current is basically controlled by the phase shift angle ¢. Therefore, the

TABLE 5 Comparison among XFC-based SST topologies [86]

Topology	Merits	Demerits	LVDC link regulation	HVDC link regulation	Size	Cost	Modularity implementation
Type-I (Figure 4a) [64, 65]	Simple control	No PFC, poor reactive power compensation	N/A	N/A	Low size due to unavailability of dc link	Low due to reduced size and filter	Simple
Type-II (Figure 4b) [67–69]	PFC, RE integration possible at the LV side	Lower efficiency, high switching losses	Good	N/A	Moderate due to more number of power devices/switches and LVDC link	Medium due to more power devices required	Hard
Type-III (Figure 4c) [71, 62]	PFC, low THD	RE integration not possible due to absence of LVDC link	N/A	Good	Moderate due to more number of power devices/switches and HVDC link	Medium due to more power devices required	Hard
Type-IV (Figure 4d) [61, 72]	Reactive power compensation, harmonic elimination	Complex control, bulky capacitors	Very good	Very Good	Large size due to presence of HVDC and LVDC link more number of power devices/switches	High due to high bulky dc links and large number of power devices/switches	Simple

TABLE 6 MV interfaced SST-based XFC prototypes

Reference	Topology/core technology	Configuration	Control	Capabilities	Testing	Efficiency (%)
[61, 88]	3.6 kV 10 kW EV fast charger (Figure 6)	ac/dc front end H-bridge, dc/dc DHB converter	PWM	Bidirectional power flow, grid voltage support, ac systems decoupling	Steady state, load unbalanced	95.2
[94]	3.8 kV 16 kW EV fast charger (Figure 8)	ac/dc TLB rectifier, half-bridge LLC dc/dc converter	PLL	Power factor correction (PFC), total harmonic distortion (THD)	Voltage regulation, input current regulation, voltage balancing	98.4
[91, 92]	3.8 kV 25 kW EV fast charger (Figure 7)	ac/dc *i*TCM topology, dc/dc LLC series resonant converter	Phase shift modulation	Bidirectional power flow, power factor correction	Calorimeter loss distribution and efficiency measurement	99.1
[83]	8 kV, 25 kW modular SST (Figure 9)	AFE 3-level ac/dc converter, dc/dc LLC converter	DSP controller	PFC, low harmonic distortion	Voltage regulation test against both load and source	97.5
[95]	2.4 kV, 50 kW modular SST (Figure 10)	3 level ac/dc boost converter, dc/dc NPC converter	Three loops PI Controller	Unidirectional, PFC, low THD, high power density	Double pulse test	96.6
[98]	12.47 kV, 350 kW modular SST	3 level boost ac/dc, dc/dc DAB converter	Triple phase shift (TPS) control method	High efficiency, low current THD, PFC	Double pulse test, voltage regulation	98.1
[99]	4.8 kV or 13.2 kV, 400 kW modular SST design	ac/dc 3 level dual NPC converter, LCL resonant dc/dc converter	Complex control due to LLC converter	Bidirectional power flow, PFC, low THD	Fixed voltage and power	96.5

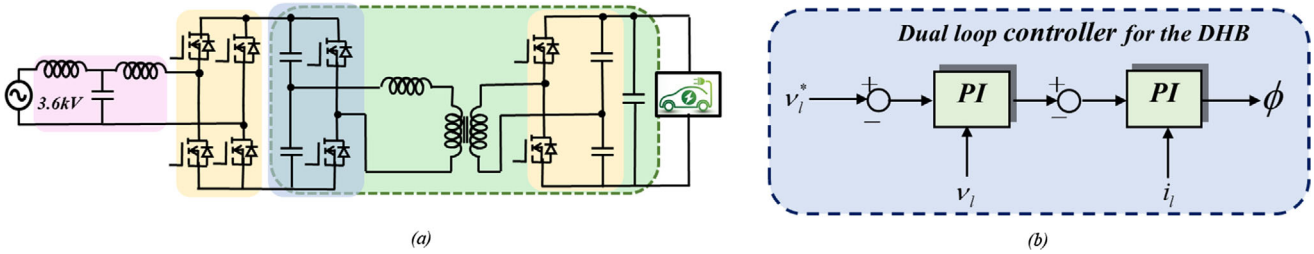

FIGURE 6 (a) 3.6 kV 10 kW EV fast charger [61], (b) control diagram [88]

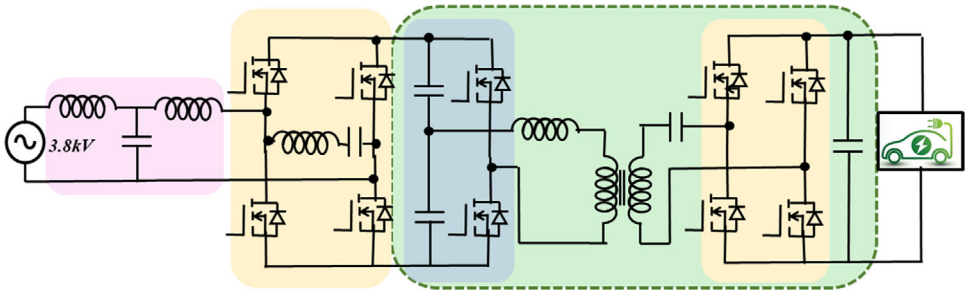

FIGURE 7 3.8 kV 25 kW EV fast charger [93, 96]

closed loop control of DHB involves two control items, an inner current loop and an outer voltage control loop [90], as illustrated in Figure 6(b). As both the controlled parameters are dc, therefore, the PI controller is used to mitigate the steady state offsets. This control strategy is responsible for voltage harmonics compensation, but higher order current harmonics are not included as they lie beyond the cut-off frequency of the LC filter. Moreover, the protection against system disturbances is accomplished through the conversion of sensor output into pulses, as mentioned in [88]. The results show that the controller is capable of performing grid side voltage restoration with a 10% voltage drop.

In [91, 92], another SiC MOSFETs based 10 kV single-module SST design is implemented for direct interfacing with the 3.8 kV MV grid (Figure 7). Similar to [88], an integrated triangular current mode (*i*TCM) converter topology is used that comprises of an ac/dc full bridge rectifier with a unipolar modulation control technique to reduce the switching losses. However, in this case, the range of switching frequency of the PWM leg lies between 35 to 75 kHz. Apart from the front-end rectifier, *i*TCM consists of an isolated dc/dc stage, which includes an LLC series resonant converter (SRC) based on 10 kV SiC MOSFETs on the MV side of HFT. The primary task of the dc/dc converter is to provide the galvanic isolation and the constant dc-link voltage level (7 kV/400 V). The voltage at the dc-link is regulated at a constant value by the front-end ac/dc rectifier of the SST, and thereby ZVS is achieved for all the MOSFETs. The variable switching frequency f_{sw} to attain a fixed value of ZVS current [93] can be found from the following function [91]:

$$f_{sw} = \frac{A\,(t)\,u_g^2}{4P\left|\sin\left(\omega_g t\right)\right| + u_g^2 I_{ZVS}}\left(\frac{1}{L_g} + \frac{1}{L_b}\right) \tag{7}$$

where

$$A\ (t) = \left|\sin\left(\omega_g t\right)\right| . \left[1 - \frac{u_g}{U_{DC}} . \left|\sin\left(\omega_g t\right)\right|\right] \tag{8}$$

Furthermore, an LC branch is inserted between the two-phase legs of PWM, which allows high switching frequency operation at MV and also limits the current harmonics according to the IEEE 519 standard. The efficiency of 25 kW, MV interfaced SST topology was measured to be 99.1%.

Another modular SST implementation [94] is given in Figure 8. This configuration uses an ac/dc front end three-level boost (TLB) circuit and half-bridge LLC converter in dc/dc stage with 1.2 kV SiC devices. At the MV side, four modules are serially connected for sharing 3.6 kV ac voltage. The voltage balancing in the system can be achieved by using LLC transformers. At 16 kW, the efficiency of the system is >98%. A

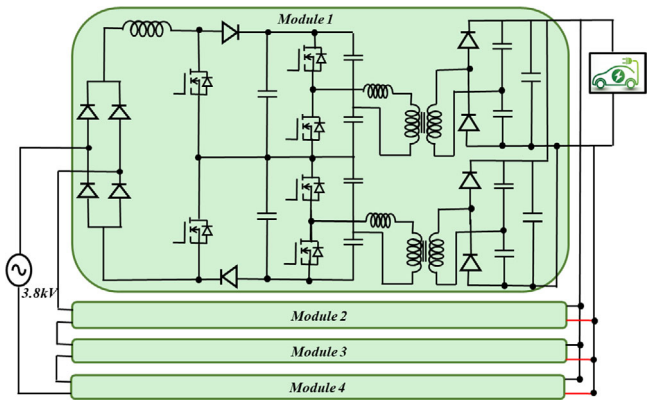

FIGURE 8 3.8 kV 16 kW EV fast charger [94]

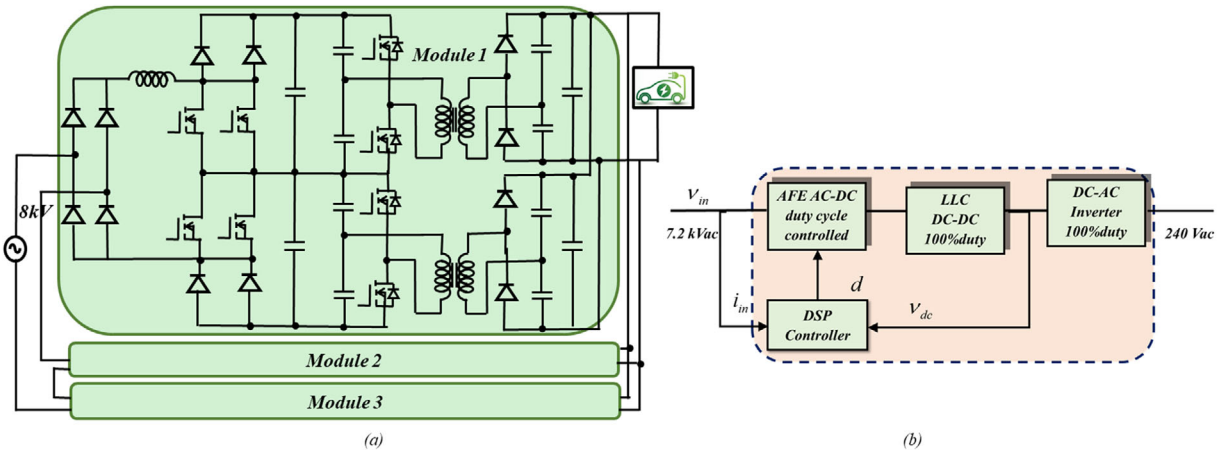

FIGURE 9 (a) 8 kV, 25 kW modular SST [83], (b) control of 8 kV, 25 kW modular SST [83]

digital control system is designed and proposed in [94] for this TLB-SST design. The control system's entire structure comprises four parts that include a phase-locked loop (PLL), PWM generators, feedback control, and ideal duty-ratio feed-forward loop. The ideal feed-forward loop is responsible for improving the input current THD at the zero-crossing.

An MV interfaced 8 kV, 25 kW modular SST was proposed in Figure 9(a) [83]. At the MV side, for sharing 8 kV ac voltage, ten modules are serially connected. The front end of each module has an uncontrolled diode rectifier bridge that is accompanied by the two parallel combinations of unidirectional active front-end (AFE) 3-level boost converter. The isolated dc/dc stage comprises two half-bridge LLC converters that are used for soft-switching. For higher efficiency, LLC converters have 100% duty cycle operation in the open-loop, while their voltage at output level is controlled by using ac/dc front end, which regulates the bus voltage. Due to the mismatching of two LLC, transformers voltage imbalance can be observed under lightly loaded conditions.

The basic closed loop control for the topology of [83] is shown in Figure 9(b). A DSP controller is used to regulate the AFE ac/dc converter that is responsible for PFC, harmonic mitigation, and voltage regulation. PFC function is applied with multiple control to ensure low THD. The general expression of a DSP feedback controller is given in Equation (9) [100, 101]:

$$G\left(z\right) = \omega_c\, G_b \frac{T_s\left(z+1\right)}{2\left(z-1\right)}\left(\frac{\omega_c T_s\left(z+1\right)+2K\left(z-1\right)}{K\omega_c T_s\left(z+1\right)+2\left(z-1\right)}\right) \tag{9}$$

where ω_c and K are represented as,

$$\omega_c = \frac{2}{T_s}\tan\left(f_c T_s \pi\right)$$

$$\text{and} \qquad K = \sqrt{\frac{\left(1+\sin\left(\left(PM-\left(90^\circ-\emptyset_b\right)\right)\frac{\pi}{180}\right)\right)}{\left(1+\sin\left(\left(PM-\left(90^\circ-\emptyset_b\right)\right)\frac{\pi}{180}\right)\right)}}$$

where f_c is the controller's crossover frequency and PM is the required phase margin at f_c. The loop gain of the digital current control loop is then derived in [b] as follows:

$$T_z = \frac{0.4035\left(z+1\right)\left(z-0.9915\right)}{z\left(z+0.8418\right)\left(z-1\right)^2} \tag{10}$$

A traditional PI controller is adopted by the dc bus for voltage regulation [83]. However, the dc bus reference varies by varying loading conditions and is scaled by the magnitude of input current. Moreover, protection against unbalancing, overloading, and short circuit is an important feature of this configuration.

Based on the topology depicted in Figure 10(a) [84, 95–97], another fast charger of 50 kW is made at North Carolina State University. At the MV side, three modules are connected in series for sharing 2.4 kV ac voltages. This design minimizes the forward voltage drop on each diode and increases its efficiency. Each module has 3-level boost converter, which is used for PFC. The successive dc/dc stage consists of a half-bridge NPC converter that further reduces the size of HFT. The control configuration for this design is given in Figure 10(b). Three loops with PI controllers are used, namely, dc bus main loop that regulates the dc bus voltage, the voltage balancing loop that regulates the capacitor voltage, and the NPC loop that controls the output voltage. This control technique is responsible for current harmonic mitigation by limiting current THD below 2% and high-power density with an overall system efficiency of 97.5%. In 2019, a similar converter configuration was adopted with a relatively higher voltage level (12.47 kV) and high power (350 kW) modular structure [98]. Per phase control scheme consisting of three loops similar to [95] is used for testing purposes. Moreover, a high-power density (1.6 kW/L) converter is designed with the system efficiency exceeds 98%.

Another SST-based 400 kW XFC implementation is given in [99]. Two different voltage levels are available, 4.8 kV with three modules and 13.2 kV with nine modules. 15 kV SiC MOSFETs are used, which gives improved system efficiency but results in a higher cost.

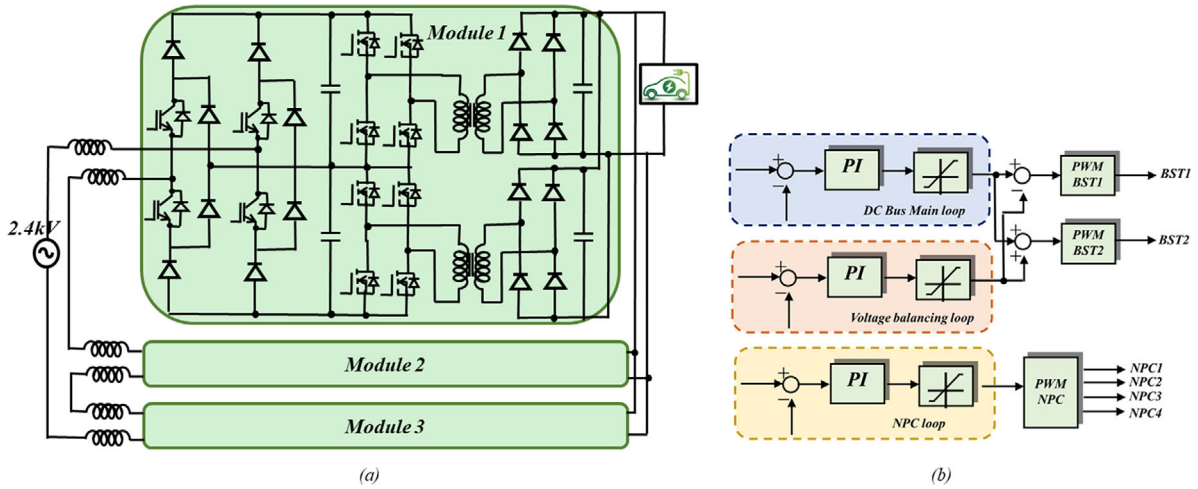

FIGURE 10 (a) For 2.4 kV, 50 kW modular SST [95], (b) basic control diagram [96]

Table 7 demonstrates a comparison of several MV interfaced SST-based dc fast chargers control techniques. Different parameters, such as voltage and current harmonics, voltage drop under varying loading conditions, dc offset load unbalances, overloads, and protection against system disturbances, are considered. It can be seen that most researches focus on the mitigation of input current THD, whereas voltage drops under varying loading conditions are the least focused parameter.

6 | FUTURE CHALLENGES AND SOLUTIONS IN ADOPTING SST-BASED XFC INFRASTRUCTURE

This section describes the current challenges and potential solutions associated with SST based XFC EV charging stations implementation.

6.1 | Future challenges

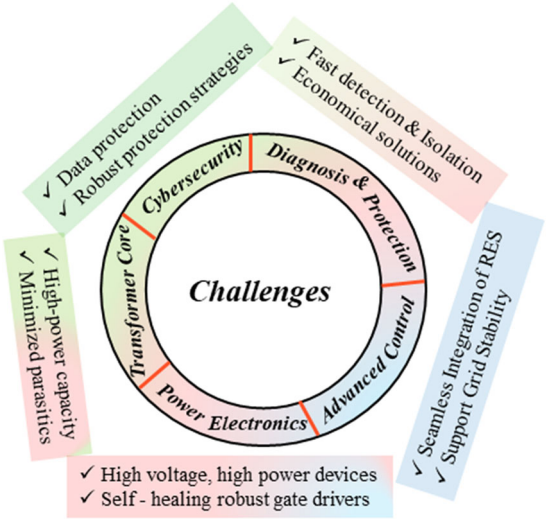

FIGURE 11 Challenges and potential solution for wide acceptance of SST

Despite various promising features of the SST-based EV XFC, such as higher efficiency, fast charging, lower installation cost, and better site utilization etc., there are some barriers to its complete adoption. The major concerns involving the integration of SST technology can be categorized into five major fields, as shown in Figure 11.

The major challenge exists in the field of power electronics, where high voltage, high power semiconductor devices must be adopted and commercialized to develop high power SSTs for EV charging. One hardware hindrance would be an improvement in the transformer core's design and implementation using superior magnetic materials. There is a limitation on the maximum power transfer possible with the existing magnetic materials with a single core (in each mode of SST). Further, one more challenge is the increased reliability and cybersecurity requirements of SST based EV implementations. It is well—known that SSTs have lower reliability compared to LFT (due to a higher number of components). This concern must be addressed for higher power deployments. Moreover, with the digitalization of dynamic grid structure, cyber threats of grid operation must be addressed for online control performance.

In addition, the adoption of SST-based EV XFC requires fast-acting protection schemes. The key technical difficulties include the lack of a suitable protection scheme and circuit breakers against short circuits, over-voltages, and overloading conditions in SST [102]. Another requirement would be the development of fast-acting communication links (for sensing, diagnosis, and protection). This also requires the implementation of faster programming devices for controlling the system. Moreover, as a modern grid is highly dynamic, grid stability and optimum control are becoming highly challenging. In this aspect, SST can contribute to improved grid performance by controlling its active-reactive power flow in accordance with the load curve. LFT with an ac/dc converter can also achieve the

TABLE 7 Comparison of control techniques of MV interfaced SST-based dc fast chargers

Reference	Topology/core technology	Control strategy	Considered controlled parameters					Summary and advantages
			Voltage harmonics	Current harmonics	Voltage drops (under varying loading conditions)	DC off-set load unbalances	Protection against system disruptions and overloads	
[61, 88]	3.6 kV 10 kW EV fast charger (Figure 6)	PWM modulation	THD about 3%	✗	✓	Steady-state	Through conversion of sensor output into pulses	Steady state operation at full load, grid voltage support, ac systems decoupling
[96]	3.8 kV 16 kW EV fast charger (Figure 8)	PLL	✗	THD at zero crossings	✗	✓	✓	Voltage regulation, input current regulation, voltage balancing
[91, 92]	3.8 kV 25 kW EV fast charger (Figure 7)	Phase shift modulation	✗	According to the IEEE 519 standard	✗	✗	✗	Calorimeter loss distribution and efficiency measurement
[83]	8 kV, 25 kW modular SST (Figure 9)	DSP controller	✓	✓	✗	Due to mismatching of LLC transformers	✓	Voltage regulation against both load and source
[95]	2.4 kV, 50 kW modular SST (Figure 10)	Three loops PI controller	✗	THD below 2%	✗	✓	✗	High power quality, high efficiency

same; however, the SST concept needs faster, predictive, and stable control, which must solve complex, contradictory optimization problems. For achieving this control, techniques must be based on advanced methods that are superior to the traditional PI based controllers. An area of challenge in this regard would be the integration of renewable energy with the existing SST/grid structure.

Furthermore, one limitation is the need for proper standards and certifications. The direct interface of power electronics converters with the MV grid does not incorporate the present EV charger standards such as CHAdeMO, GB/T, CSS Type 1, and 2. Therefore, in addition to the available standards, other power quality certifications and standards are required for MV instrumentation [103, 104]. Another concern would be the life safety issues of EV owners and other related personnel handling the EV infrastructure.

6.2 | Solutions/opportunities

Experience of SST implementation from other fields (traction-based implementations) can be used to improve the confidence level and maturity of the technology. The commercialization and development of high-power semiconductor devices are in progress. SiC and GaN based devices having 6.5 kV ratings are also introduced in the market. However, commercial-scale products with robust self-healing gate driver circuits must be developed to enhance the performance, protection, and isolation of fast-acting SSTs. Improved transformer core power handling capability is also in progress. It mainly involves the realization of HFT with superior magnetic materials. However, the realization of the cores in SST by stacking multiple individual core segments has been done regularly [105]. Also, the parasitics or non-linearities of the transformer must be minimized to avoid any EMI/over-voltage issues occurring due to high switching frequency operation.

SSTs can provide compatibility with the power systems having high penetration of RESs and distributed energy storage (DERs) by utilizing the approach of DC microgrids (MGs). The use of SST in control of these MGs with various DC loads, such as EVs, helps in increasing the overall efficiency of power systems by reducing the conversion stages [106, 107]. An example of such an architecture is proposed in [108], using SST, known as a zonal microgrid. It maintains the stability and power quality of the MG by utilizing maximum power from RESs and PVs.

For improving the reliability aspect of SST based systems, robust communication and data protection protocols must be developed. The development of highly encrypted communication channels with high-level security is in the development stages for microgrid operations. SSTs can be added as an additional component in the development stage for wider acceptance in the future. Protection schemes for MV power electronics-based SSTs are proposed and reported by FRREDM lab [109]. Moreover, the SST-based solution is utilizing its capability of reactive power compensation in the power system for the elimination of transient fault [110]. Furthermore, whenever a fault occurs at the distribution line, an uninterrupted power

supply is provided by the RESs connected with the SST, thereby ensures continuous power supply to the connected load [26].

The operation of SST at higher frequencies requires faster communication and control platforms. With the existing technology, control platforms having 10 ns step size (100 MHz) are available using high-end FPGAs. However, synchronization of different FPGA boards (required for control of complex systems) may limit the application of the minimum step size. With the improvement in the control platforms in the last decade, the development of faster devices looks inevitable, thereby helping the SST implementations. However, issues such as EMI noise due to high frequency power signals must be accordingly addressed.

Despite the promising benefits and several substantial potential solutions of the SST-based EV fast charging, a considerable pushback from the industry and society is seen to fully adopt this new concept with converters directly connected to the MV line. However, there is a need to deploy more pilot XFC stations to emphasize the utility and industrial benefits, which is a reasonable first step toward the complete adoption of SST-based solutions.

7 | CONCLUSION

In this paper, a comprehensive comparison of using traditional LFT and HFT is presented. The overall cost and size of SST are comparatively less than LFT. The state-of-art SST topologies for dc fast chargers provide higher efficiency, size and cost reduction, galvanic isolation, and better site utilization over the existing EV fast charger topologies. In addition to the step-down function, the SST-based solution provides reactive power control, better power quality performance and voltage regulation, and easy integration of RESs. With the adoption of SST, XFC can mimic the refuelling experience of gasoline vehicles. Four different emerging topologies of the SST-based solution are presented, out of which the most SSTs adopt the type IV topology to provide an optimized performance in the context of size, weight, volume, and efficiency. A comprehensive comparison among various control techniques is made, showing the control type, considered mitigation factors, and their benefits. An overview of the current challenges, including protection, metering, standardization, and certification, and their potential solutions in the complete adoption of SST based charging solutions are also discussed.

ACKNOWLEDGMENTS

This publication was made possible by UREP grant # [27-021-2-010] from the Qatar National Research Fund (a member of the Qatar Foundation). The statements made herein are solely the responsibility of the authors. The Article Processing Fee of this article is paid by the Qatar National Library.

REFERENCES

1. Fernández, G., et al.: EV charging infrastructure in a petrol station, lessons learned. In: 2018 International Symposium on Industrial Electronics, INDEL 2018 – Proceedings. Banja Luka (2019)
2. Ghavami, M., Singh, C.: Reliability evaluation of electric vehicle charging systems including the impact of repair. In: 2017 IEEE Industry Applications Society Annual Meeting. Cincinnati, OH, pp. 1–9 (2017)
3. Wang, Y., et al.: The scale, structure and influencing factors of total carbon emissions from households in 30 provinces of China-Based on the extended STIRPAT model. Energies 11(5), 1125 (2018)
4. New ZOE - 100% Electric & Versatile City Car - Renault UK. https://www.renault.co.uk/electric-vehicles/zoe.html (2020). Accessed on October 23, 2020
5. Model 3 | Tesla. https://www.tesla.com/model3 (2020). Accessed Oct 2020
6. Chery eQ1 EV | Specs | Range | Battery | Charge Time | Price | WattEV2Buy. https://wattev2buy.com/electric-vehicles/chery-auto/chery-eq1-ev-electric-car/ (2020). Accessed Oct 2020
7. Ronanki, D., Kelkar, A., Williamson, S.S.: Extreme fast charging technology-prospects to enhance sustainable electric transportation. Energies 12(19), 3721 (2019)
8. Srdic, S., Lukic, S.: Toward extreme fast charging: challenges and opportunities in directly connecting to medium-voltage line. IEEE Electrif. Mag. 7(1), 22–31 (2019)
9. Haghbin, S., et al.: Integrated chargers for EV's and PHEV's: Examples and new solutions. In: 19th International Conference on Electrical Machines, ICEM 2010. Rome, Italy (2010)
10. Grenier, M., et al.: Design of onboard charger for plug-in hybrid electric vehicle. In: 5th IET International Conference on Power Electronics, Machines and Drives (PEMD 2010). Brighton, UK, pp. 1–10 (2010)
11. Radimov, N., et al.: Three-stage SiC-based bi-directional onboard battery charger with titanium level efficiency. IET Power Electron. 13(7), 1477–1480 (2020)
12. Yilmaz, M., Krein, P.T.: Review of integrated charging methods for plug-in electric and hybrid vehicles. In: 2012 IEEE International Conference on Vehicular Electronics and Safety, ICVES. Istanbul, Turkey, pp. 346–351 (2012)
13. Singh, B., et al.: A review of three-phase improved power quality ac-dc converters. IEEE Trans. Ind. Electron. 51(3), 641–660 (2004)
14. Fasugba, M.A., Krein, P.T.: Gaining vehicle-to-grid benefits with unidirectional electric and plug-in hybrid vehicle chargers. In: 2011 IEEE Vehicle Power and Propulsion Conference, VPPC 2011. Chicago (2011)
15. Liu, C., et al.: Opportunities and challenges of vehicle-to-home, vehicle-to-vehicle, and vehicle-to-grid technologies. Proc. IEEE 101(11), 2409–2427 (2013)
16. Joseph, P.K., Devaraj, E., Gopal, A.: Overview of wireless charging and vehicle-to-grid integration of electric vehicles using renewable energy for sustainable transportation. IET Power Electron. 12(4), 627–638 (2019)
17. Habib, S., Kamran, M., Rashid, U.: Impact Analysis of Vehicle-To-Grid Technology and Charging Strategies of Electric Vehicles on Distribution Networks - A Review. Elsevier B.V., Amsterdam. vol. 277, 205–214 (2015)
18. Chen, H., Wang, X., Khaligh, A.: A single stage integrated bidirectional AC/DC and DC/DC converter for plug-in hybrid electric vehicles. In: 2011 IEEE Vehicle Power and Propulsion Conference, VPPC 2011. Chicago (2011)
19. Du, Y., et al.: Review of high power isolated bi-directional DC-DC converters for PHEV/EV DC charging infrastructure. In: IEEE Energy Conversion Congress and Exposition: Energy Conversion Innovation for a Clean Energy Future. ECCE 2011, Proceedings. Phoenix, AZ, pp. 553–560 (2011)
20. Zhou, X., et al.: Design and control of grid-connected converter in bi-directional battery charger for plug-in hybrid electric vehicle application. In: 5th IEEE Vehicle Power and Propulsion Conference, VPPC '09. Dearborn, MI, pp. 1716–1721 (2009)
21. Zhou, X., et al.: Multi-function bi-directional battery charger for plug-in hybrid electric vehicle application. In: 2009 IEEE Energy Conversion Congress and Exposition, ECCE 2009. San Jose, CA, pp. 3930–3936 (2009)
22. Dharmakeerthi, C.H., Mithulananthan, N., Saha, T.K.: Impact of electric vehicle fast charging on power system voltage stability, Int. J. Electr. Power Energy Syst. 57, 241–249 (2014)

23. Tu, C., et al.: Research of the high supply voltage quality control for solid-state transformer. IET Power Electron. 11(11), 1–8 (2018)
24. 1547a-2020 - 1547a-2020 - IEEE Standard for Interconnection and Interoperability of Distributed Energy Resources with Associated Electric Power Systems Interfaces–Amendment 1: To Provide More Flexibility for Adoption of Abnormal Operating Performance Category III - IEEE Standard. https://ieeexplore.ieee.org/abstract/document/9069495 (2020). Accessed Oct 2020
25. Kolar, J.W., Huber, J.E.: Solid-State Transformers - Key Design Challenges, Applicability, and Future Concepts. In: 17th International Conference on Power Electronics and Motion Control (PEMC 2016). Varna, Bulgaria (2016)
26. She, X., Huang, A.Q., Burgos, R.: Review of solid-state transformer technologies and their application in power distribution systems. IEEE J. Emerging Sel. Top. Power Electron. 1(3), 186–198 (2013)
27. Huang, A.Q.: Medium-voltage solid-state transformer: Technology for a smarter and resilient grid. IEEE Ind. Electron. Mag. 10(3), 29–42 (2016)
28. Apostolaki-Iosifidou, E., Codani, P., Kempton, W.: Measurement of power loss during electric vehicle charging and discharging. Energy 127, 730–742 (2017)
29. Huber, J.E., Kolar, J.W.: Applicability of solid-state transformers in today's and future distribution grids. IEEE Trans. Smart Grid 10(1), 317–326 (2019)
30. Tu, H., et al.: Extreme fast charging of electric vehicles: A technology overview. IEEE Trans. Transp. Electrif. 5(4), 861–878 (2019)
31. Suarez, C., Martinez, W.: Fast and ultra-fast charging for battery electric vehicles – A review. In: 2019 IEEE Energy Conversion Congress and Exposition (ECCE). Baltimore, MD, pp. 569–575 (2019)
32. Rare Look Inside Tesla Supercharger. https://insideevs.com/news/322486/rare-look-inside-tesla-supercharger/ (2020). Accessed October 2020
33. Yilmaz, M.; Krein, P.T.: Review of battery charger topologies, charging power levels, and infrastructure for plug-in electric and hybrid vehicles. IEEE Trans. Power Electron 28, 2151–2169 (2013)
34. Khaligh, A., D'Antonio,: Global trends in high-power on-board chargers for electric vehicles. IEEE Trans. Veh. Technol. 68, 3306–3324 (2019)
35. Habib, S., et al.: A comparative study of electric vehicles concerning charging infrastructure and power levels. In: Proceedings - 2017 International Conference on Frontiers of Information Technology, FIT 2017. Islamabad, pp. 327–332 (2017)
36. CHAdeMO. https://www.chademo.com/chademo-3-0-released/. Accessed on October 30, 2020
37. Yan, J., et al.: Model predictive control-based fast charging for vehicular batteries. Energies 4(8), 1178–1196 (2011)
38. Liu, C., Liu, L.: Optimizing battery design for fast charge through a genetic algorithm based multi-objective optimization framework. ECS Trans. 77(11), 257 (2017)
39. Mai, W., Colclasure, A.M., Smith, K.: Model-instructed design of novel charging protocols for the extreme fast charging of lithium-ion batteries without lithium plating. J. Electrochem. Soc. 167(8), 080517 (2002)
40. Xavier, MA., Trimboli, M.S: Lithium-ion battery cell-level control using constrained model predictive control and equivalent circuit models. J. Power Sources 285, 374–384 (2015)
41. Goldar, A., et al.: MPC strategies based on the equivalent hydraulic model for the fast charge of commercial Li-ion batteries. Comput. Chem. Eng. 141, 107010 (2020)
42. Dusmez, S., Cook, A., Khaligh, A.: Comprehensive analysis of high quality power converters for level 3 off-board chargers. In: 2011 IEEE Vehicle Power and Propulsion Conference, VPPC 2011. Chicago (2011)
43. IEC 61851-1:2017 - Electric vehicle conductive charging system - Part 1: General requirements. https://standards.iteh.ai/catalog/standards/iec/c472de67-e272-4734-9103-cf9f4725c597/iec-61851-1-2017 (2020). Accessed Oct 2020
44. EN 61851-23:2014 - Electric vehicle conductive charging system - Part 23: DC electric vehicle charging station. https://standards.iteh.ai/catalog/standards/clc/114bd98a-e033-4c5d-9bdc-4f8de579cc34/en-61851-23-2014 (2020). Accessed Oct 2020
45. IEC 61851-24; Electric vehicle conductive charging system - Part 24: Digital communication between a d.c. EV charging station and an electric vehicle for control of d.c. charging › Research Explorer. https://cris.vub.be/en/publications/iec-6185124-electric-vehicle-conductive-charging-system–part-24-digital-communication-between-a-dc-ev-charging-station-and-an-electric-vehicle-for-control-of-dc-charging(75962181-050a-40ec-99c5-1b4745db679f)/export.html (2020). Accessed Oct 2020
46. Tritium VEEFIL-RT 50KW DC FAST CHARGER. Tritium Pty Ltd 2019. https://www.tritium.com.au/product/productitem?url=veefil-rt-50kwdc-fast-charger (2020). Accessed 20 Dec 2018
47. Tritium LAUNCHING SOON- VEEFIL-PK DC ULTRA-FAST CHARGER 175 kW- 475 kW. Tritium Pty Ltd 2019. https://www.tritium.com.au/veefillpk (2018). Accessed 22 Dec 2018.
48. CHAdeMO. https://www.chademo.com/portfolios/takaoka-charger-09/. Accessed on September 20, 2020.
49. Phihong 'Phihong EV Chargers, ' Phihong 2017. https://www.phihong.com.tw/newcatalog/2017%20EV%20Chargers%20%E5%86%8A%E5%AD%90_20170420_EN.pdf (2018). Accessed 22 Dec 2018
50. Alatalo, M.: Module size investigation on fast chargers for BEV. Swedish Electromobility Centre. https://emobilitycentre.se/wp-content/uploads/2018/08/Module-sizeinvestigation-on-fast-chargers-for-BEV-final.pdf (2018). Accessed 22 Dec 2018
51. EVteQ, 'SET-QM EV Charging Module'. https://www.evteqglobal.com/product-details/set-qm-evcharging-module (2017). Accessed 22 Dec 2018
52. ABB 'High Power Charging' ABB. https://new.abb.com/ev-charging/products/car-charging/high-powercharging (2018). Accessed 22 Dec 2018
53. Abu-Siada, A., Budiri, J., Abdou, A.: Solid state transformers topologies, controllers, and applications: State-of-the-art literature review. Electronics 7(11), 298 (2018)
54. Avdeev, B., Vyngra, A., Chernyi, S.: Improving the electricity quality by means of a single-phase solid-state transformer. Designs 4(3), 35 (2020)
55. Huber, J.E., Kolar, J.W.: Volume/weight/cost comparison of a 1MVA 10 kV/400 V solid-state against a conventional low-frequency distribution transformer. In: 2014 IEEE Energy Conversion Congress and Exposition, ECCE 2014. Pittsburgh, PA, pp. 4545–4552 (2014)
56. 'Delta', https://www.deltaww.com/en-US/products/EV-Charging/4865. Accessed on October 02, 2020
57. 'ABB', https://search.abb.com/library/Download.aspx?DocumentID=9AKK107680A7994&LanguageCode=en&DocumentPartId=&Action=Launch. Accessed on October 02, 2020.
58. 'Delta', https://3814f048-6c69-488c-9f3ee8df0a79bfd4.filesusr.com/ugd/1667b4_ed598c2eeea34ffd9d792ba156c78710.pdf. Accessed on October 02, 2020.
59. Rhombus Energy Solutions. https://rhombusenergysolutions.com/wp-content/uploads/2020/02/Rhombus-500kW-EV-Charger-datasheet-v4-010220.pdf. Accessed on October 02, 2020.
60. Muratori, M., et al.: Technology solutions to mitigate electricity cost for electric vehicle DC fast charging. Appl. Energy 242, 415–423 (2019)
61. Wang, F., et al.: Design and operation of A 3.6kV high performance solid state transformer based on 13kV SiC MOSFET and JBS diode. In: 2014 IEEE Energy Conversion Congress and Exposition, ECCE 2014. Pittsburgh, PA, pp. 4553–4560 (2014)
62. Sabahi, M., et al.: Zero-voltage switching bi-directional power electronic transformer. IET Power Electron. 3(5), 818–828 (2010)
63. Brando, G., Dannier, A., deo Pizzo, A.: A simple predictive control technique of power electronic transformers with high dynamic features. In: 5th IET International Conference on Power Electronics, Machines and Drives (PEMD 2010). Brighton, UK, pp. 1–6 (2010)
64. Qin, H., Kimball, J.W.: Ac-Ac dual active bridge converter for solid state transformer. In: 2009 IEEE Energy Conversion Congress and Exposition, ECCE 2009. San Jose, CA, pp. 3039–3044 (2009)
65. Chen, H., Prasai, A., Divan, D.: Dyna-C: A minimal topology for bidirectional solid-state transformers. IEEE Trans. Power Electron. 32(2), 995–1005 (2017)

66. Qin, H., Kimball, J.W.: Solid-state transformer architecture using AC-AC dual-active-bridge converter. IEEE Trans. Ind. Electron. 60(9), 3720–3730 (2013)
67. Carpita, M., et al.: Multi-level converter for traction applications: Small-scale prototype tests results. IEEE Trans. Ind. Electron. 55(5), 2203–2212 (2008)
68. Drábek, P., et al.: New configuration of traction converter with medium-frequency transformer using matrix converters. IEEE Trans. Ind. Electron. 58, 5041–5048 (2011)
69. Hugo, N., et al.: Power electronics traction transformer. In: 2007 European Conference on Power Electronics and Applications, EPE. Barcelona, Spain (2007)
70. She, X., et al.: Review of solid state transformer in the distribution system: From components to field application. In: 2012 IEEE Energy Conversion Congress and Exposition, ECCE 2012. Raleigh, NC, pp. 4077–4084 (2012)
71. Banaei, M.R., Salary, E.: Power quality improvement based on novel power electronic transformer. In: 2011 2nd Power Electronics, Drive Systems and Technologies Conference, PEDSTC 2011. Tehran, Iran, pp. 286–291 (2011)
72. Fan, H., Li, H.: High-frequency transformer isolated bidirectional DC-DC converter modules with high efficiency over wide load range for 20 kVA solid-state transformer. IEEE Trans. Power Electron. 26(12), 3599–3608 (2011)
73. Kimura, N., et al.: Solid state transformer investigation for HVDC transmission from offshore windfarm. In: 2017 IEEE 6th International Conference on Renewable Energy Research and Applications (ICRERA). San Diego, CA, pp. 574–579 (2017)
74. Madhusoodhanan, S., et al.: Solid-state transformer and MV grid tie applications enabled by 15 kV SiC IGBTs and 10 kV SiC MOSFETs based multilevel converters. IEEE Trans. Ind. Appl. 51(4), 3343–3360 (2015)
75. Parseh, N., Mohammadi, M.: Solid state transformer (SST) interfaced doubly fed induction generator (DFIG) wind turbine. In: 2017 25th Iranian Conference on Electrical Engineering, ICEE 2017. Tehran, Iran, pp. 1084–1089 (2017)
76. Zhang, Z., et al.: Voltage and power balance control strategy for three-phase modular cascaded solid stated transformer. In: Conference Proceedings - IEEE Applied Power Electronics Conference and Exposition – APEC. Long Beach, CA, pp. 1475–1480 (2016)
77. Chetri, C., et al.: Study of various design for SST implementation. Int. J. Sci. Res. Eng. Dev. no date, 3. 3(1), 1–8 (2020)
78. Mostafa, M.A., et al.: SBO-based selective harmonic elimination for nine levels asymmetrical cascaded H-bridge multi-level inverter. Aust. J. Electr. Electron. Eng. 15(3), 131–143 (2018)
79. Mostafa, M.A., Abdou, A.F., El-Gawad, A.F.A., El-Kholy, E.E.: Comparison of multi-carrier and SHE-PWM for a nine levels cascaded H-bridge inverter. In: 2017 19th International Middle-East Power Systems Conference, MEPCON 2017 – Proceedings. Cairo, Egypt, pp. 1483–1491 (2018)
80. Priya, M., Ponnambalam, P., Muralikumar, K.: Modular-multilevel converter topologies and applications – A review. IET Power Electron. 12, 170–183 (2019)
81. Fast, Utility Direct Medium Voltage DC. "Charger Update: DC Fast Charger Characterization." *EPRI, Palo Alto, CA: Dec* 1024016 (2012).
82. Sedaghati, F., et al.: Analysis and implementation of a modular isolated zero-voltage switching bidirectional dc-dc converter. IET Power Electron. 7(8), 2035–2049 (2014)
83. Lai, J.S., et al.: A 15-kV class intelligent universal transformer for utility applications. In: Conference Proceedings - IEEE Applied Power Electronics Conference and Exposition – APEC. Long Beach, CA, pp. 1974–1981 (2016)
84. Srdic, S., et al.: A SiC-based high-performance medium-voltage fast charger for plug-in electric vehicles. In: ECCE 2016 - IEEE Energy Conversion Congress and Exposition, Proceedings. Milwaukee (2016)
85. Vasiladiotis, M., Rufer, A.: A modular multiport power electronic transformer with integrated split battery energy storage for versatile ultra-fast EV charging stations. IEEE Trans. Ind. Electron. 62(5), 3213–3222 (2015)
86. Hannan, M.A. et al.: State of the art of solid-state transformers: Advanced topologies, implementation issues, recent progress and improvements. IEEE Access 8, 19113–19132 (2020)
87. Mcmurray, William. "Power converter circuits having a high frequency link." U.S. Patent 3,517,300, issued June 23, 1970.
88. Wang, F., et al.: A 3.6kV high performance solid state transformer based on 13kV SiC MOSFET. In: 2014 IEEE 5th International Symposium on Power Electronics for Distributed Generation Systems, PEDG 2014. Galway, Ireland (2014)
89. Andersson, D., Carlsson, D.: Measurement of ABB s prototype fast charging station for electric vehicles. M.S. Thesis. Chalmers University of Technology, Sweden (2012).
90. Krismer, F., Kolar, J.W.: Accurate small-signal model for the digital control of an automotive bidirectional dual active bridge. IEEE Trans. Power Electron. 24(12), 2756–2768 (2009)
91. Rothmund, D., et al.: 99.1% Efficient 10 kV SiC-based medium-voltage ZVS bidirectional single-phase PFC AC/DC stage. IEEE J. Emerging Sel. Top. Power Electron. 7(2), 779–797 (2019)
92. Rothmund, D., et al.: 99% Efficient 10 kV SiC-based 7 kV/400 v DC transformer for future data centers. IEEE J. Emerging Sel. Top. Power Electron. 7(2), 753–767 (2019)
93. Rothmund, D., et al.: 10kV SiC-based bidirectional soft-switching single-phase AC/DC converter concept for medium-voltage solid-state transformers. In: 2017 IEEE 8th International Symposium on Power Electronics for Distributed Generation Systems, PEDG 2017. Florianopolis, Brazil (2017)
94. Lee, M., et al.: Modeling and control of three-level boost rectifier based medium-voltage solid-state transformer for DC fast charger application. IEEE Trans. Transp. Electrif. 5(4), 890–902 (2019)
95. Srdic, S., et al.: A SiC-based power converter module for medium-voltage fast charger for plug-in electric vehicles. In: Conference Proceedings - IEEE Applied Power Electronics Conference and Exposition – APEC. Long Beach, CA, pp. 2714–2719 (2016)
96. Liang, X., et al.: Predictive control of a series-interleaved multicell three-level boost power-factor-correction converter. IEEE Trans. Power Electron. 33(10), 8948–8960 (2018)
97. Rothmund, D., Ortiz, G., Kolar, J.W.: SiC-based unidirectional solid-state transformer concepts for directly interfacing 400V DC to medium-voltage AC distribution systems. In: INTELEC, International Telecommunications Energy Conference (Proceedings). Vancouver, BC (2014)
98. Liang, X., et al.: A 12.47 kV Medium Voltage Input 350 kW EV Fast Charger using 10 kV SiC MOSFET. In: 2019 IEEE Applied Power Electronics Conference and Exposition (APEC). Anaheim, CA, pp. 581–587 (2019)
99. Zhu, C.: High-Efficiency, Medium-Voltage-Input, Solid-State Transformer-Based 400-kW/1000-V/400-A Extreme Fast Charger for Electric Vehicles. https://www.energy.gov/sites/prod/files/2019/06/f64/elt241_zhu_2019_o_4.24_9.31pm_jl.pdf. Accessed on August 10, 2020
100. Cho, Y., Miwa, H., Lai, J.: A digital single-loop control of multi-phase dc-dc converter for fuel cell powered truck auxiliary power unit. In: 8th International Conference on Power Electronics - ECCE Asia. Jeju, pp. 2261–2266 (2011)
101. Cho, Y., Mok, H., Lai, J.S.: Analysis of the admittance component for digitally controlled single-phase bridgeless PFC converter. J. Power Electron. 13(4), 600–608 (2013)
102. Guillod, T., et al.: Protection of MV/LV solid-state transformers in the distribution grid. In: IECON 2015 - 41st Annual Conference of the IEEE Industrial Electronics Society. Yokohama, Japan, pp. 3531–3538 (2015)
103. 519-2014 - 519–2014 - IEEE Recommended Practice and Requirements for Harmonic Control in Electric Power Systems - Redline - IEEE Standard. https://ieeexplore.ieee.org/document/7047985 (2020). Accessed Oct 2020
104. IEEE Xplore Full-Text PDF. https://ieeexplore.ieee.org/stamp/stamp.jsp?arnumber=7048070 (2020). Accessed Oct 2020
105. Nguyen-Duy, K., et al.: Minimization of the transformer inter-winding parasitic capacitance for modular stacking power supply applications. In:

2014 16th European Conference on Power Electronics and Applications, EPE-ECCE Europe 2014. Lappeenranta, Finland (2014)
106. Borgaonkar, Aumkar. "Solid state transformers: A review of technology and applications." *Indian Inst. Technol., New Delhi, India, Tech. Rep* (2015).
107. Rahman, S., Khan, I.A., Amini, M.H.: A review on impact analysis of electric vehicle charging on power distribution systems. In: 2020 2nd International Conference on Smart Power & Internet Energy Systems (SPIES). Bangkok, Thailand, pp. 420–425 (2020)
108. She, X., et al.: On integration of solid-state transformer with zonal DC microgrid. IEEE Trans. Smart Grid 3(2), 975–985 (2012)
109. Tatcho, P., Jiang, Y., Li, H.: A novel line section protection for the FREEDM system based on the solid state transformer. In: IEEE Power and Energy Society General Meeting. Detroit, MI (2011)
110. She, X., et al.: Wind energy system with integrated functions of active power transfer, reactive power compensation, and voltage conversion. IEEE Trans. Ind. Electron. 60(10), 4512–4524 (2013)

How to cite this article: Tahir, Y., et al.: A state-of-the-art review on topologies and control techniques of solid-state transformers for electric vehicle extreme fast charging. IET Power Electron. 14, 1560–1576 (2021). https://doi.org/10.1049/pel2.12141